The Journal of Physiology

Regulation of microRNA-221, -222, -21 and -27 in articular cartilage subjected to abnormal compressive forces

Paulina S. Stadnik[1], Sophie J. Gilbert[1], Jessica Tarn[2], Sarah Charlton[2], Andrew J. Skelton[2], Matthew J. Barter[2], Victor C. Duance[1], David A. Young[2] and Emma J. Blain[1]

[1] *Biomechanics and Bioengineering Research Centre Versus Arthritis, Biomedicine Division, School of Biosciences, The Sir Martin Evans Building, Cardiff University, Cardiff, Wales, UK*
[2] *Skeletal Research Group, Institute of Genetic Medicine, Newcastle University, Newcastle upon Tyne, UK*

Edited by: Michael Hogan & Alicia D'Souza

Key points

- microRNAs (miRs) are small non-coding molecules that regulate post-transcriptional target gene expression.
- miRs are involved in regulating cellular activities in response to mechanical loading in all physiological systems, although it is largely unknown whether this response differs with increasing magnitudes of load.
- miR-221, miR-222, miR-21-5p and miR-27a-5p were significantly increased in *ex vivo* cartilage explants subjected to increasing load magnitude and in *in vivo* joint cartilage exposed to abnormal loading.
- *TIMP3* and *CPEB3* are putative miR targets in chondrocytes
- Identification of mechanically regulated miRs that have potential to impact on tissue homeostasis provides a mechanism by which load-induced tissue behaviour is regulated, in both health and pathology, in all physiological systems.

Abstract MicroRNAs (miRs) are small non-coding molecules that regulate post-transcriptional target gene expression and are involved in mechano-regulation of cellular activities in all physiological systems. It is unknown whether such epigenetic mechanisms are regulated in response to increasing magnitudes of load. The present study investigated mechano-regulation of miRs in articular cartilage subjected to 'physiological' and 'non-physiological' compressive loads *in vitro* as a model system and validated findings in an *in vivo* model of abnormal joint loading. Bovine full-depth articular cartilage explants were loaded to 2.5 MPa (physiological) or 7 MPa (non-physiological) (1 Hz, 15 min) and mechanically-regulated miRs identified using next generation sequencing and verified using a quantitative PCR. Downstream targets were verified using miR-specific mimics or inhibitors in conjunction with 3′-UTR luciferase activity assays.

Dr Sophie Gilbert has worked in the connective tissue field for 25 years focussing on the relationship between biomechanics and biology of joint tissues. She has extensive research experience in extracellular matrix biology in normal and disease states including its epigenetic regulation under mechanical load. She has been pivotal in developing and characterising cell and animal models to investigate the signalling mechanisms that drive mechanical load and inflammation induced joint pathology. These include a novel, and recently published, anterior cruciate ligament (ACL) rupture model of post-traumatic osteoarthritis which in 2018 received the award for "Excellence in Basic, Clinical, and Translational Science" bestowed by the Journal of Orthopaedic Research. Her goal is to elucidate potential mechanisms of joint destruction that may be targeted in the treatment or diagnosis of arthritis.

DOI: 10.1113/JP279810

A subset of miRs were mechanically-regulated in *ex vivo* cartilage explants and *in vivo* joint cartilage. miR-221, miR-222, miR-21-5p and miR-27a-5p were increased and miR-483 levels decreased with increasing load magnitude. Tissue inhibitor of metalloproteinase 3 (*TIMP3*) and cytoplasmic polyadenylation element binding protein 3 (*CPEB3*) were identified as putative downstream targets. Our data confirm miR-221 and -222 mechano-regulation and demonstrates novel mechano-regulation of miR-21-5p and miR-27a-5p in *ex vivo* and *in vivo* cartilage loading models. *TIMP3* and *CPEB3* are putative miR targets in chondrocytes. Identification of specific miRs that are regulated by increasing load magnitude, as well as their potential to impact on tissue homeostasis, has direct relevance to other mechano-sensitive physiological systems and provides a mechanism by which load-induced tissue behaviour is regulated, in both health and pathology.

(Received 20 April 2020; accepted after revision 9 October 2020; first published online 14 October 2020)
Corresponding author E. J. Blain: Biomechanics and Bioengineering Research Centre Versus Arthritis, Biomedicine Division, School of Biosciences, The Sir Martin Evans Building, Cardiff University, Museum Avenue, Cardiff, CF10 3AX, Wales, UK. Email: blain@cardiff.ac.uk

Introduction

Mechanical loading is essential with respect to regulating the functional capabilities of physiological systems including the musculoskeletal, cardiovascular and nervous system; this is achieved, at the cell and tissue level, by adapting to changes in mechanical load and/or metabolic stress applied. One of the major musculoskeletal tissues, articular cartilage, primarily functions to dissipate mechanical forces across the synovial joint surface and facilitates smooth, low-friction movement. The biomechanical integrity of articular cartilage is reliant on the biochemical composition of the extracellular matrix (ECM) (Gilbert & Blain, 2018), and maintenance of cartilage tissue homeostasis, effected by the chondrocytes, is similarly dependent on mechanical load (Buckwalter *et al.* 2005). Joint articular cartilage is predominantly exposed to dynamic compressive forces, although both tensile strain and shear stresses also result from everyday movement (Lee *et al.* 2005). Application of moderate, physiological mechanical loads is essential for maintaining cartilage homeostasis by promoting anabolic activities such as increased production of ECM molecules, whereas abnormal, non-physiological joint loading, as characterized by either overload or insufficient load, disrupts the homeostatic balance, favouring catabolism and cartilage degeneration, comprising the hallmark of osteoarthritis (OA) (Felson, 2013).

Mechano-regulation of cellular activities within physiological systems is known to occur through epigenetic mechanisms (e.g. RNA silencing). Primary contributors to RNA silencing are the microRNAs (miR), which are small (20–2 3bp), non-coding cytoplasmic RNAs that control the post-transcriptional regulation of one-third of all genes and are important in development, homeostasis and degeneration of tissues, including articular cartilage (Goldring & Marcu, 2012). Epigenetic studies have demonstrated that mechanical force has an impact on cellular responses through regulation of miR expression levels in tendon fibroblasts (Mendias *et al.* 2012), smooth muscle cells (Song *et al.* 2012), trabecular meshwork cells (Luna *et al.* 2011) and endothelial cells (Qin *et al.* 2010; Weber *et al.* 2010; Zhou *et al.* 2011). A small number of miRs were also identified as being mechanosensitive in chondrocytes (Dunn *et al.* 2009; Guan *et al.* 2011; Jin *et al.* 2014; Yang *et al.* 2016; Cheleschi *et al.* 2017). However, these studies were performed on isolated cells devoid of a substantial ECM, a feature known to be critical for cell–matrix mechano-communications (Guilak *et al.* 2006).

Therefore, using articular cartilage as a model system, the present study aimed to identify miRs that respond to 'physiological' and 'non-physiological' mechanical loads and to investigate the regulation of their potential downstream target genes.

Materials and methods

Reagents were from Sigma (Poole, UK) unless otherwise specified; molecular biology reagents and plastic ware were certified RNase and DNase-free. Culture medium consisted of Dulbecco's modified Eagle's medium/Ham's F12-glutamax (1:1; Life Technologies, Paisley, UK) supplemented with 100 μg mL^{-1} penicillin, 100 U mL^{-1} streptomycin, 50 μg mL^{-1} ascorbate-2-phosphate and 1 × insulin-transferrin-selenium ethanolamine (1 × ITS-X; Life Technologies).

Preparation of articular cartilage explants and high-density primary chondrocytes

Full depth articular cartilage explants were removed (5 mm biopsy punch; Selles Medical Limited, Hull, UK) from the metacarpophalangeal joint of <3-week old bovine calves within 6 h of slaughter (F. Drury & Sons Abattoir, Swindon, UK); ethical approval was not required. Cartilage explants were equilibrated in culture medium for 3 days prior

to mechanical load. Primary chondrocytes were isolated from full depth cartilage utilizing the same tissue source as explants, and enzymatic digestion was performed (Al-Sabah *et al.* 2016). All cultures were maintained in 5% CO_2 and 20% O_2 at 37°C. Each experiment utilized tissue from between two and three animals, and repeat experiments utilized tissue from independent animals.

In vitro application of mechanical load to cartilage explants

Cartilage explants were subjected to either a 'physiological' (2.5 MPa, 1 Hz) or a 'non-physiological' load (7 MPa, 1 Hz) for 15 min using the ElectroForce 3200 (TA Instruments, New Castle, DE, USA) (Al-Sabah *et al.* 2016) and gene expression analysed at 2, 6 and 24 h post-load; unloaded explants served as controls. Explants were immediately snap frozen and remained in liquid nitrogen (<48 h) until RNA extraction. Loading regimes were selected based on articular cartilage literature demonstrating that ≤5 MPa is generally accepted as a 'physiological' load (Grodzinsky *et al.* 2000; Fehrenbacher *et al.* 2003), whereas peak loads >5 MPa are considered degradative (i.e. 'non-physiological') (Fehrenbacher *et al.* 2003); the frequency was set at 1 Hz, which has been demonstrated to resemble a human fast walking speed (Bader *et al.* 2011).

In vivo application of mechanical load

Twelve-week old male C57Bl6 mice (~25 g; Envigo, Huntington, UK) were randomly assigned to either experimental or control groups and randomly allocated to MB1 cages (960 cm^2) in groups of five (12:12 h light/dark photocycles, with food and water available *ad libitum*). Animal husbandry and procedures were performed in compliance with the Animals (Scientific Procedures) Act 1986 [Home Office licence P287E87DF] according to Home Office and ARRIVE guidelines (Kilkenny *et al.* 2010). Mice were anaesthetized with isoflurane and custom-built cups used to hold the right ankle and knee in flexion with a 30° offset prior to the application of a 0.5 N pre-load (ElectroForce13200; TA Instruments, Elstree, UK). A single 12 N load at a velocity of 1.4 mm s^{-1} was then applied resulting in anterior cruciate ligament (ACL) rupture as described previously (Gilbert *et al.* 2018); mechanical loading was always conducted in the morning. Buprenorphine (0.05 mg kg^{-1}) was administered S.C. to mice at the start of the experiment; animals were able to move freely and were monitored for welfare and lameness until termination of the experiment. Mice were culled by cervical dislocation at either day 1 or 7 post-load and the knee articular cartilage was dissected and processed for histology (toluidine blue staining) as described previously (Gilbert *et al.* 2018) or immediately snap frozen and remained in liquid nitrogen until RNA extraction. These early time points allowed assessment of mechanically regulated miRs in cartilage prior to overt degenerative changes and ECM loss. Nine animals were utilized for quantification of miR levels and the representative histology depicting the loading model phenotype is derived from experiments published in Gilbert *et al.* (2018).

RNA extraction and reverse transcription for mRNA analysis

Total RNA was extracted from cartilage explants/chondrocytes using 500 μL of Trizol reagent (Invitrogen, Paisley, UK) (Al-Sabah *et al.* 2016). RNA integrity was assessed (2100 Bioanalyzer and associated RNA 6000 Nano kit; Agilent Technologies, Wokingham, UK) and RNA integrity numbers >8.5 were observed. cDNA (total volume of 20 μL) was synthesized from 300 ng of total RNA using Superscript III reverse transcriptase in conjunction with 0.5 μg of random primers (Promega, Southampton, UK) in accordance with the manufacturer's instructions (Invitrogen).

RNA extraction and reverse transcription for miR analysis

Total RNA was extracted from cartilage explants/chondrocytes as described above, except 1 mL of Trizol reagent was used. After ethanol precipitation, total RNA was purified using a mirVana miR Isolation Kit (Ambion, Paisley, UK) in accordance with the manufacturer's instructions. RNA integrity numbers of >8.0 were observed. cDNA of mature miRs was generated separately from total RNA (5 ng) using the TaqMan MicroRNA Reverse Transcription Kit (Applied Biosystems, Paisley, UK) involving 50 U of MultiScribe Reverse Transcriptase and stem-looped reverse transcription primers, specific to individual miRs, from TaqMan MicroRNA Assays (Applied Biosystems, Paisley, UK) in accordance with the manufacturer's instructions.

miR next generation sequencing and bioinformatic analysis

Mechanically-regulated articular cartilage miRs were identified using next generation sequencing (NGS) using >3.5 μg of RNA per sample. Procedures were conducted in accordance with the manufacturers' instructions. Library preparation was conducted on 450 ng of total RNA using the NEB Next Small RNA Library Prep Set for Illumina (Multiplex Compatible: BioLabs, Hitchin, UK) and amplified cDNA was purified using a QIAquick PCR

Purification Kit (Qiagen, Crawley, UK). miR libraries were selected by running purified cDNA samples on 8% (v/v) polyacrylamide gels and excising bands located at ∼140 bp (Crowe *et al.* 2016). A Multiplex Compatible kit (NEB Next Small RNA Library Prep Set for Illumina) was used to elute and purify the miRs, and the concentration of miR libraries assessed prior to analysis on a HiSeq Sequencing System (The Genome Analysis Centre, Norwich, UK). miR deep sequencing data (raw FASTQ files) were run through FastQC and Cutadapt (Martin 2011), and trimmed FASTQ files were aligned against known *bos taurus* miR sequences from miRBase (http://www.mirbase.org). Quantification was determined by counting aligned reads against a reference, using a combination of RSamTools and ShortRead (Li *et al.* 2009) bioconductor packages. Differential expression was assessed using DESeq2 (Love *et al.* 2014). Global experimental variance was analysed using principal component analysis to assess for outlier samples and statistical significance from differential expression tests was determined by retaining miRs that had an adjusted $P < 0.05$.

Manipulation of miR expression levels in high-density chondrocyte cultures

Primary bovine chondrocytes were seeded onto six-well culture plates (VWR, Lutterworth, UK) at a density of 4×10^6 cells per well in antibiotic-free culture media and incubated at 37°C for 24 h prior to transfection. Chondrocytes were transfected for 48 h with 50 nM mirVana miR inhibitors (Applied Biosystems) or 50 nM miScript miR mimics (Qiagen) using DharmaFECT1 lipid reagent (Dharmacon, Cambridge, UK) in accordance with the manufacturer's instructions; mirVana miR Inhibitor Negative Control #1 (Applied Biosystems) and AllStars negative control small interfering RNA (siRNA) (Qiagen) were utilized as transfection controls (50 nM).

Quantification of miRNA and mRNA transcripts

Quantification of mRNA or miR in experimental samples was performed using a MxPro3000 QPCR system (Agilent Technologies, Stockport, UK) and measured using either reference gene primers (MWG-Biotech AG, Ebersberg, Germany) or bovine-specific TaqMan probes (Applied Biosystems, Paisley, UK) in conjunction with either Brilliant III Ultra-Fast SYBR Green QPCR Master Mix (Agilent Genomics, Berkshire, UK) or TaqMan Fast Advanced Master Mix (Applied Biosystems, Paisley, UK). Reference gene primers (200 nM final concentration (Al-Sabah *et al.* 2016)) including SDHA, YWHAZ, HPRT, 18 s and β-actin were validated as per MIQE guidelines (Bustin *et al.* 2009). Cycling conditions were: 95°C-3 min (1 cycle), 95°C-15 s followed by 60°C-30 s (40 cycles) with an additional dissociation cycle of 95°C-1min, 60°C-30 s followed by 95°C-30 s (1 cycle) to confirm primer specificity with SYBR Green detection. Relative quantification was calculated using the $2^{-\Delta\Delta}$CT method (Livak & Schmittgen, 2001), with unloaded controls as a reference group to quantify relative changes in transcript expression. Fold change was normalized to the geometric mean of 2–3 reference genes whose expression was identified as stable under the experimental condition using RefFinder software (https://www.heartcure.com.au/for-researchers/).

Luciferase activity assays

The 3′-UTR of mRNAs, containing the predicted binding site of target miRs, were cloned into pmirGLO dual-luciferase miRNA target expression vector (Promega, Southampton, UK) by In-Fusion (Takara Bio Europe, Saint-Germain-en-Laye, France) and construct sequences verified (for primer sequences, see Table 1). SW1353 chondrosarcoma cells (∼20 000 cells cm^{-2}) were co-transfected with 50 nM miRNA mimics with the reporter plasmids (500 ng mL^{-1}) (Barter *et al.* 2015); transfection of 50 nM AllStars negative control siRNA with the reporter plasmids was used as control. Following a 24 h transfection, cells were lysed and luciferase levels were determined using a Promega GloMax luminometer and the Dual-Luciferase reporter assay system (Promega).

Statistical analysis

Quantitative PCR (qPCR) data are presented as the mean ± 95% confidence intervals (CIs) after normalization to identified reference genes for explants (*SDHA* and *YWHAZ*), transfected cells (*HPRT* and *YWHAZ*) or *in vivo* model (*U6*, *18s* and *β-actin*) and further normalized to untreated controls. Experiments were performed on explants ($n = 6$), transfected cells ($n = 3$) and *in vivo* studies ($n = 9$), with three independent repeats for explant and cell studies. Data were assessed for normality and differences in variances and transformed where required. One-way ANOVA and Fisher's *post hoc* test were performed to determine significance of mechanical load or manipulation of miR expression levels on gene expression, respectively; the results were considered statistically significant at $P < 0.05$ (Minitab, version 17; Minitab, LLC, State College, PA, USA).

Results

Identification and validation of mechanically-regulated miRs in cartilage explants

NGS was performed on cartilage explants subjected to a 2.5 or 7 MPa load (1 Hz, 15 min) to identify mechano-sensitive

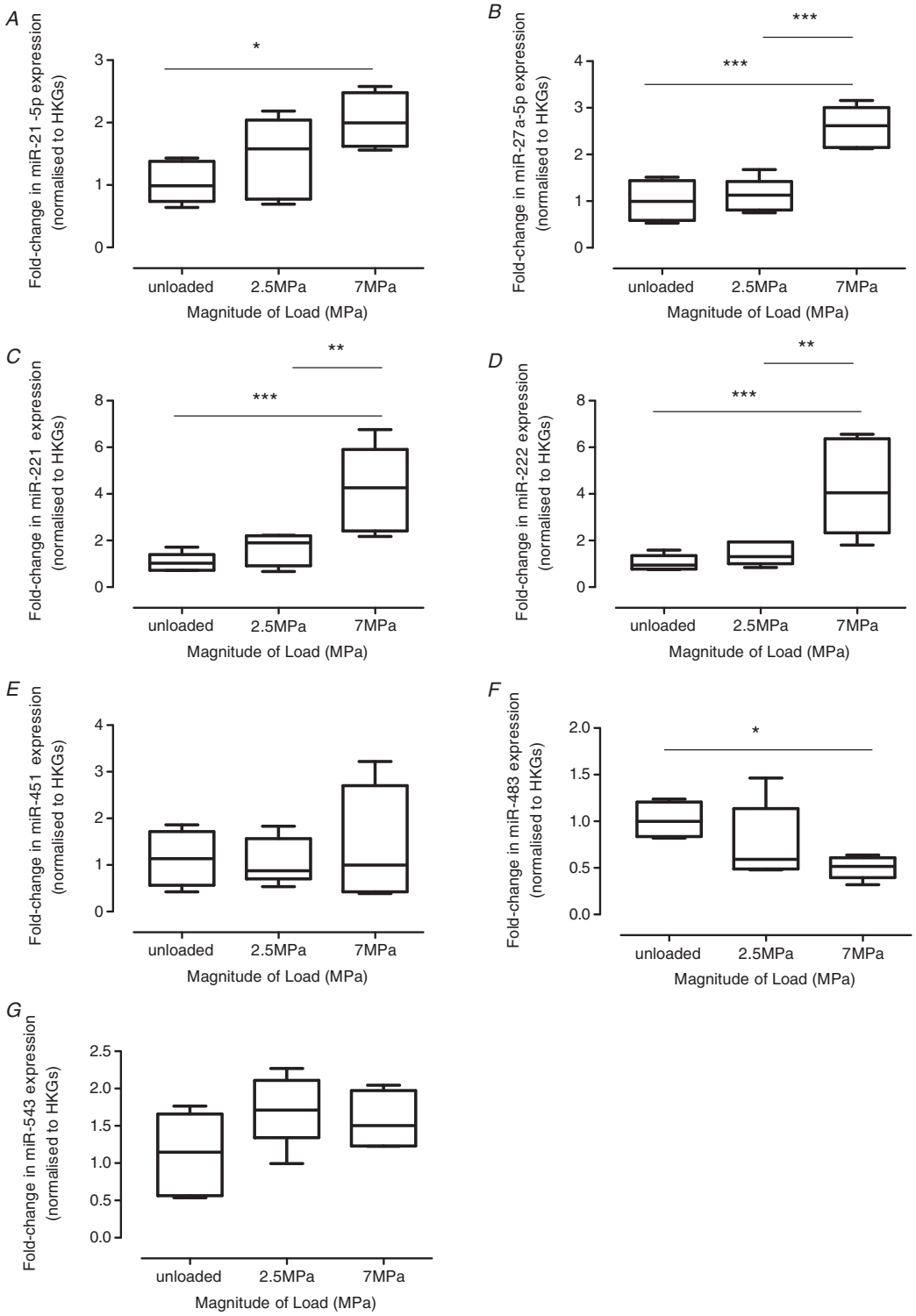

Figure 1. Validation of mechanically-regulated miRs in cartilage explants using qPCR
qPCR validation of mechanically-regulated miRs, identified by NGS, in cartilage explants subjected to loads of 2.5 or 7 MPa (1 Hz, 15 min) and analysed 24 h post-cessation of load for (*A*) miR-21-5p, (*B*) miR-27a-5p, (*C*) miR-221, (*D*) miR-222, (*E*) miR-451, (*F*) miR-483 and (*G*) miR-453; unloaded explants served as controls. miR levels were normalized to the geometric mean of two reference genes (*SDHA*, *YWHAZ*) and further normalized relative to the unloaded control cDNAs. Data are presented as box plots depicting the mean ± 95% CI ($n = 6$ explants) and are representative of three independent experiments. Statistical analysis was performed using one-way ANOVA with Tukey's *post hoc* test.

Table 1. Sequences of primers used to clone the 3′-UTR of mRNAs containing the predicted binding site of target miRs

Target	5′- to 3′ Oligo sequence	Annealing temperature (°C)
TIMP3	F 5′-GCTCGCTAGCCTCGACTGAGCTTCCCTTGGACACT-3′ R	60
UTR	5′-CGACTCTAGACTCGAGCTAAAGGGAAAGGCGGAT-3′	
CPEB3	F 5′-GCTCGCTAGCCTCGAAAGGAGGGAAAAGAGAGGGC-3′ R	60
UTR	5′-CGACTCTAGACTCGAAACAGAGCACCGCAAAGTAC-3′	

Table 2. Mean fold-change and statistical significance of mechanically-regulated miRs in articular chondrocytes subjected to loads of 2.5 or 7 MPa (1 Hz, 15 min), to represent a physiological or non-physiological load respectively, and analysed 2, 6 and 24 h post-cessation of load (unloaded explants served as controls)

	UL *vs*. 2.5MPa		UL *vs*. 7MPa		2.5 *vs*. 7MPa	
	FC	*P*adj	*FC*	*P*adj	*FC*	*P*adj
Analysed 2 h post-cessation of load						
miR-27a-5p	4.420	2.79×10^{-22}	7.092	3.08×10^{-40}		
miR-2898	0.588	0.008	0.408	3.16×10^{-10}		
miR-2478			0.566	0.001		
miR-98			1.698	0.001		
miR-23b-3p			1.539	0.004		
miR-1260b			0.647	0.025		
miR-23a			1.464	0.034		
miR-148b			1.644	0.039		
Analysed 6 h post-cessation of load						
miR-486	0.521	0.002				
miR-677			2.149	5.50×10^{-5}	1.933	0.001
miR-222			1.568	0.008		
miR-2889					2.393	1.54×10^{-6}
miR-1249					0.562	0.013
Analysed 24 h post-cessation of load						
miR-222	1.814	0.003	7.409	8.81×10^{-51}	4.085	4.00×10^{-25}
miR-27a-5p			3.019	1.14×10^{-16}	2.027	5.84×10^{-7}
miR-221			3.393	1.63×10^{-13}	2.593	3.58×10^{-8}
miR-543			2.619	1.30×10^{-9}	1.725	0.005
miR-21-5p			2.267	6.67×10^{-6}	1.719	0.013
miR-495			1.775	1.45×10^{-4}		
miR-451			0.481	0.002		
miR-425-5p			0.626	0.010	0.672	0.037
miR-20a			1.603	0.012		
miR-7			1.699	0.017		
miR-760-3p			1.715	0.017		
miR-2318			1.8518	0.022		
miR-2344			1.829	0.030		
miR-431			1.817	0.030		
miR-155			1.472	0.042		
miR-100			1.429	0.048		
miR-483					0.599	0.025

Data are representative of three independent experiments ($n = 6$ explants per individual experiment).

miRs (Table 2); unloaded explants served as controls. NGS analysis was conducted at 2, 6 or 24 h post-load to investigate temporal differences in miR expression. A small number of annotated miRs were significantly regulated by load at 2 h (8 miRs) (Table 2) and 6 h (5 miRs) (Table 2), with 17 miRs detected at 24 h post-load (Table 2). A greater number of miRs were only regulated by the non-physiological 7 MPa load (Table 2). Given the number of significant changes at 24 h post-load (Table 2), the top five most significantly up-regulated (i.e.

miR-222, -27a-5p, -221, -543 and -21-5p) and the two most significantly down-regulated (i.e. miR-451 and -483) were validated for this time point using TaqMan qPCR on individual RNA samples (Fig. 1). Relative to unloaded, a 7 MPa load increased expression of miR-21-5p (two-fold; $P = 0.034$) (Fig. 1*A*), miR-27-5p (2.56-fold; $P = 0.001$) (Fig. 1*B*), miR-221 (3.85-fold; $P < 0.001$) (Fig. 1*C*) and miR-222 (3.78-fold; $P < 0.001$) (Fig. 1*D*), and decreased miR-483 expression (two-fold; $P = 0.047$) (Fig. 1*F*). A loading magnitude-dependent regulation of miRs was observed between explants subjected to a 7 MPa *vs.* 2.5 MPa load: miR-27-5p (2.4-fold, $P < 0.001$) (Fig. 1*B*), miR-221 (2.55-fold, $P = 0.011$) (Fig. 1*C*) and miR-222 (2.83-fold, $P = 0.002$) (Fig. 1*D*). Although miR-seq indicated that a 7 MPa load down-regulated miR-451 levels (2.1-fold, $P = 0.002$) (Table 2) and up-regulated miR-543 levels (2.62-fold, $P < 0.001$; $P = 0.005$) (Table 2) relative to unloaded cartilage, this was not verified using qPCR (Fig. 1*E* and *G*).

In vivo validation of miR-21-5p, miR-27-5p, miR-221 and miR-222 mechano-regulation

The physiological relevance of identified mechanically-regulated miRs was determined in a murine *in vivo* model of post-traumatic OA, in which ACL rupture induces mechanical instability, by applying an abnormal load to the knee joint (Gilbert *et al.* 2018). Synovial infiltration occurs rapidly followed by extensive joint degeneration as characterized by articular cartilage loss and bone remodelling by day 21 (Fig. 2*A*) (Gilbert *et al.* 2018). However, at the earlier stages analysed in the present study, the articular cartilage is intact. Of the original miRs identified (Table 1), four that were successfully validated by qPCR (miR-221, -222, -21-5p and -27-5p) (Fig. 1) were subsequently analysed *in vivo*. No significant effects were detected after 1 day of destabilization; however, after 7 days of mechanical instability, miR-221 (2.20-fold, $P < 0.001$) (Fig. 2*B*), miR-222 (1.56-fold, $P = 0.070$) (Fig. 2*C*), miR21-5p (4.75-fold, $P = 0.002$) (Fig. 2*D*) and miR-27-5p (4.21-fold, $P = 0.003$) (Fig. 2*E*) were up-regulated compared to naïve mice (control). Furthermore, miR-221 (2.05-fold, $P = 0.003$) (Fig. 2*B*), miR-222 (1.90-fold, $P = 0.030$) (Fig. 2*C*), miR21-5p (7.99-fold, $P = 0.001$) (Fig. 2*D*) and miR-27-5p (3.19-fold, $P = 0.013$) (Fig. 2*E*) were all significantly up-regulated compared to mice after 1 day of joint instability.

miR target gene validation

Potential miR target genes identified by NGS were determined using Targetscan (http://www.targetscan.org) in conjunction with an assessment of their relevance to mechanical load or cartilage homeostasis as determined using the literature; putative target genes were examined by manipulation of expression levels using specific miR mimics or inhibitors (Fig. 3). Three putative miR-21-5p targets were selected: cytoplasmic polyadenylation element binding protein 3 (*CPEB3*), matrix metalloproteinase 13 (*MMP13*) and tissue inhibitor of metalloproteinase 3 (*TIMP3*). miR-221 and miR-222 seed sites are identical; hence, the selected putative target genes included: *CPEB3*, leukaemia inhibitory factor receptor (*LIFR*) and *TIMP3*. miR-27a target gene validation was not performed because a consistent reduction in miR-27a expression was not achieved using specific antagomirs. qPCR analysis confirmed that mimic-induced elevations in miR-221 levels resulted in a significant reduction in *TIMP3* ($P = 0.006$) (Fig. 3*A*). Conversely, inhibition of miR-221 expression correlated with a significant increase in *TIMP3* transcription ($P = 0.003$) (Fig. 3*B*). Similarly, a mimic-induced increase in miR-222 levels led to a significant reduction in *TIMP3* ($P = 0.006$) (Fig. 3*C*). Conversely, inhibition of miR-222 expression correlated with a significant increase in *TIMP3* ($P = 0.025$) (Fig. 3*D*). No other putative target genes were robustly regulated by miR-221 or 222. Mimic-induced miR-21 levels resulted in a significant reduction in *TIMP3* ($P = 0.006$) (Fig. 3*E*) and *CPEB3* transcription ($P = 0.015$) (Fig. 3*G*). Conversely, inhibition of miR-21 expression correlated with a significant increase in *TIMP3* ($P = 0.010$) (Fig. 3*F*) and no significant effect on *CPEB3* ($P = 0.068$) (Fig. 3*H*). *MMP13* expression was not consistently regulated by miR-21 (data not shown).

Activation of the 3′-UTR of target mRNAs containing the predicted seed sites was investigated (Fig. 4). Addition of miR-21 mimic significantly suppressed luciferase activity regulated by *TIMP3* ($P = 0.053$) (Fig. 4*A*) and Cpeb3 3′-UTRs ($P = 0.010$) (Fig. 4*B*). Furthermore, miR-222 mimic also significantly inhibited *CPEB3* 3′-UTR regulated luciferase activity ($P = 0.010$) (Fig. 4*B*). Surprisingly, and in contrast to qPCR validation, miR-222 overexpression significantly increased luciferase activity regulated by *TIMP3* 3′-UTR ($P = 0.030$) (Fig. 4*A*). Although this contradicts the miR-222 mimic data demonstrating a significant *TIMP3* reduction (Fig. 3*C*), it does substantiate the load-induced *TIMP3* observed in the *in vitro* loading model where *TIMP3* transcription was elevated in response to 7 MPa load (4.8-fold, $P < 0.001$) (Fig. 4*C*).

Discussion

Physiological forces are critical for maintaining tissue homeostasis, and the involvement of epigenetic mechanisms such as mechano-regulation of miR expression occurs in many tissues, including articular cartilage (Dunn *et al.* 2009; Guan *et al.* 2011; Jin *et al.* 2014; Yang *et al.* 2015; Cheleschi *et al.* 2017). However, our understanding of miR involvement in

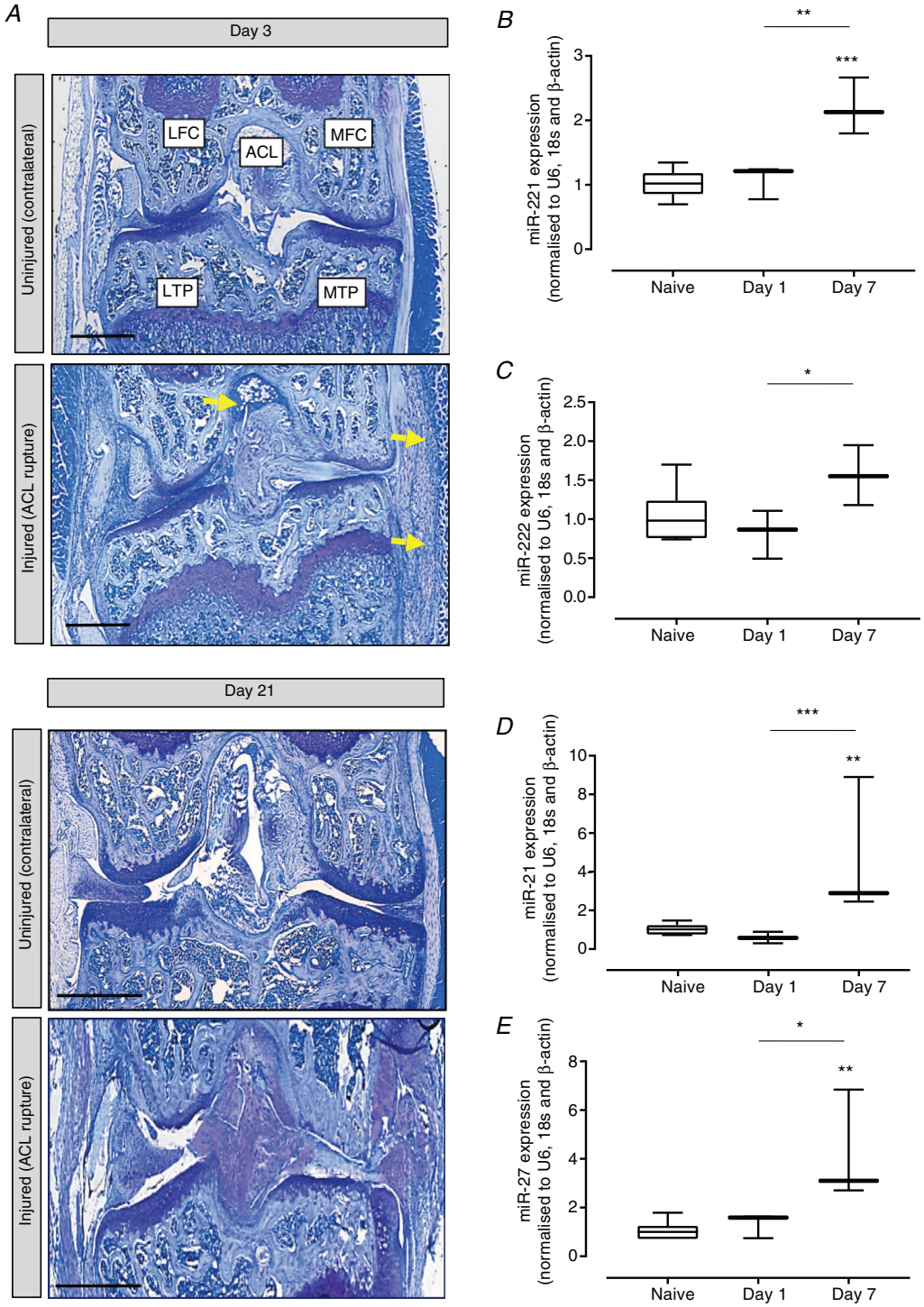

Figure 2. Validation of mechanically regulated miRNAs in a murine *in vivo* model of load-induced joint degeneration
A, toluidine blue staining of a representative mouse knee joint at days 3 and 21 after ACL rupture to induce joint instability/joint degeneration. MTP, medial tibial plateau; MFC, medial femoral condyle; LTP, tibial plateau; LFC, lateral femoral condyle; ACL, anterior cruciate ligament. Yellow indicates inflammatory cell infiltrate. Validation of differential expression of (*B*) miR-221, (*C*) miR-222, (*D*) miR-21-5p and (*E*) miR-27-5p in articular cartilage after normalization to the geometric mean of the reference genes *U6*, *β-actin* and *18s* and further normalization to the uninjured knee cartilage. Data are presented as box plots depicting the mean ± 95% CI ($n = 3$ animals per experimental time point). Statistical analysis was performed using one-way ANOVA with Tukey's *post hoc* test. [Colour figure can be viewed at wileyonlinelibrary.com]

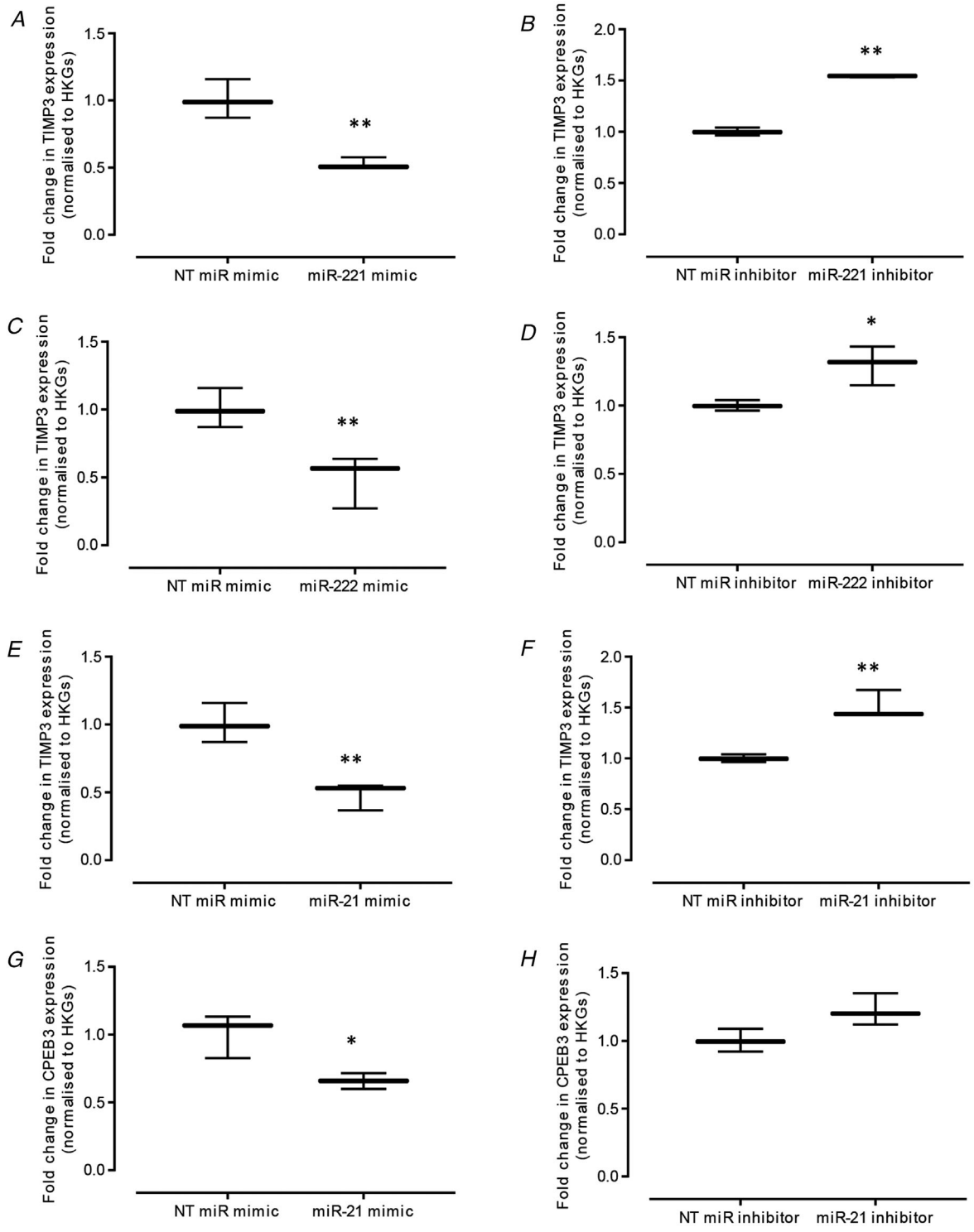

Figure 3. Validation of *TIMP3* and *CPEB3*, putative target genes of miR-221, miR-222 or miR-21, using TaqMan qPCR

Primary bovine chondrocytes were treated with either 50 nM miR mimic, 50 nM inhibitor or negative control siRNAs for each respective miR for 48 h, prior to analysis of the effect of overexpression and knockdown of miR-221 on *TIMP3* transcription (*A* and *B*), miR-222 on *TIMP3* transcription (*C* and *D*), and miR-21 on *TIMP3* (*E* and *F*) and *CPEB3* (*G* and *H*) transcript levels after normalization to the geometric mean of the reference genes *HPRT* and *YWHAZ* and further normalization to respective negative control siRNAs. Data are presented as the mean ± 95% CI ($n = 3$ wells) and are representative of three independent experiments. Statistical analysis was performed using one-way ANOVA with Tukey's *post hoc* test.

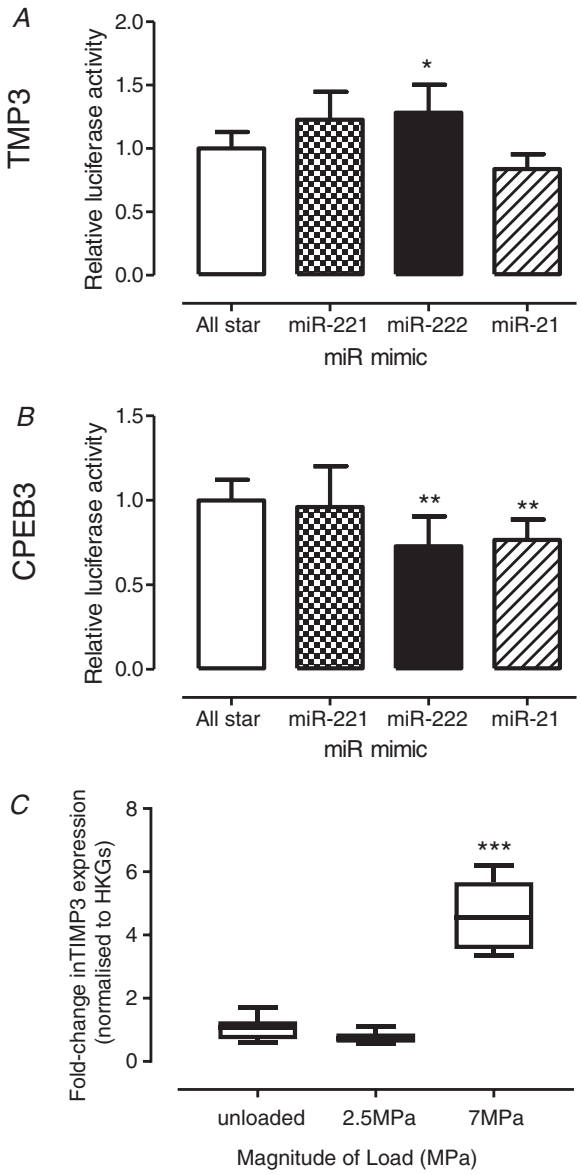

Figure 4. Verification of 3′-UTR activation of target mRNAs containing the predicted miR seed sites using a luciferase promoter assay
SW1353 chondrosarcoma cells were co-transfected with reporter plasmids containing either (*A*) *TIMP3* or (*B*) *CPEB3* 3′-UTRs and 50 nM miR-221, miR-222 or miR-21-5p mimics, or the negative control siRNA, for 24 h and luciferase levels were determined. Data are presented as the mean ± 95% CI ($n = 3$ wells) and are representative of three independent experiments. *C*, *TIMP3 m*RNA levels, as assessed using qPCR, in cartilage explants subjected to loads of 2.5 or 7 MPa (1 Hz, 15 min) and analysed 24 h post-cessation of load; unloaded explants served as controls. mRNA levels were normalized to the geometric mean of two reference genes (*SDHA*, *YWHAZ*) and further normalized relative to the unloaded control cDNAs. Data are presented as box plots depicting the mean ± 95% CI ($n = 6$ explants) and are representative of three independent experiments. Statistical analysis was performed using one-way ANOVA with Tukey's *post hoc* test.

response to different magnitudes of mechanical forces and, specifically, its impact on controlling mechanically induced tissue homeostasis is still in its infancy. The present study investigated the mechano-regulation of miRs in articular cartilage tissue explants subjected to 'physiological' and 'non-physiological' loads *in vitro* and validated regulated miRs in a murine *in vivo* model of abnormal joint loading. In addition, the study identified downstream miR targets to provide insight on mechanisms of mechanically mediated cartilage homeostasis. Importantly, the seed regions of the miRs of interest analysed in the present study are evolutionarily conserved across bovine, mouse and human species, indicating their potential physiological relevance.

Analysis of the miR-seq data illustrated that (i) a miR-mediated response to a 15 min loading episode was most noticeable at 24 h post-load and (ii) differentially regulated miRs were largely responsive to non-physiological compressive loads; the small number of miRs that were significantly regulated in response to physiological load probably reflects the loading regimen period. The miRs that were identified and validated to be most robustly altered by non-physiological load compared to unloaded controls and to physiological load were miR-221 and miR-222. This confirms the mechano-sensitive nature of miR-221 and miR-222, previously shown in cardiomyocytes after cardiac overload (El-Armouche *et al.* 2010), as well as in tendon fibroblasts (Mendias *et al.* 2012), engineered cartilage constructs in response to a catabolic loading regimen (Hecht *et al.* 2019) and anterior weight-bearing cartilage relative to the posterior non-weight bearing tissue in bovine stifle joints (Dunn *et al.* 2009).

Chondrogenic markers *COL2A1* and *SOX9* have been identified as putative gene targets for miR-221 and miR-222 (conserved seed site) that may influence cartilage homeostasis (Lolli *et al.* 2014); furthermore, miR-221 silencing strongly enhanced *in vivo* cartilage repair (Lolli *et al.* 2016). miR-221 inhibition also enhanced expression of chondrocyte-like phenotypic markers in intervertebral disc cells (Penolazzi *et al.* 2018). Therefore, miR-221 and miR-222 induction, observed in the cartilage explants in response to non-physiological load (Al Sabah A., Duance V. C., Blain E. J., unpublished observations), suggests an attempt to remodel the cartilage tissue to confer a more appropriate biomechanical response.

Analysis of downstream target genes identified robust regulation of *TIMP3* only. However, although *TIMP3* was clearly regulated via overexpression/inhibition studies in primary chondrocytes, this did not reflect observations in the SW1353 chondrosarcoma cell line for 3′-UTR activity using the luciferase assay or recapitulate events in tissue demonstrating that other, as yet unidentified, targets are regulated by miR-221 and miR-222 to elicit effects. These conflicting findings may be explained by the

different experimental systems used in the present study, thus potentially masking the effects of other regulatory contributors with respect to the influence of miR-221 and miR-222 on Timp3 expression. Another possibility that might explain the simultaneous elevation of both the tested miRs and *TIMP3* is a regulatory loop , such that elevated *TIMP3* expression induces higher expression of these miRs to reduce Timp3 transcript levels in cells over time. Analysis at time points beyond 24 h post-load would provide insight as to whether potential regulatory loops exist.

Two other miRs robustly regulated by a magnitude-dependent load in our *in vitro* and *in vivo* loading models were miR-21-5p and miR-27a-5p. To the best of our knowledge, this is the first report of the mechano-regulation of these miRs in articular cartilage. However, miR-21 mechano-regulation occurs in other cell types; tensile strain induced miR-21 expression in human aortic smooth muscle cells (Song *et al.* 2012), and both laminar (Weber *et al.* 2010) and oscillatory shear stress (Zhou *et al.* 2011) elevated miR-21 levels in human umbilical vein endothelial cells. By contrast, pulsatile shear stress inhibited miR-21 expression in these endothelial cells (Zhou *et al.* 2011), revealing the mechano-sensitive nature of these molecules. In the present study, both *TIMP3* and *CPEB3* were identified as downstream targets of miR-21-5p; however, as noted previously, *TIMP3* is not negatively correlated with miR-21-5p levels in our model systems. Furthermore, *CPEB3* levels were not significantly regulated in the present study, indicating that, although these genes are direct targets of miR-21-5p in primary chondrocytes, they are not directly regulated in our models. As a result of the complexities of such signalling mechanisms in the tissue, further experiments are clearly required to determine the interplay of these miRs and their mechanistic activities in cartilage homeostasis, which both remain beyond the scope of the present study.

miR-27a-5p was robustly regulated by mechanical load both *in vitro* and *in vivo*. Mechano-regulation of miR-27a in articular cartilage is a novel finding and corroborates studies demonstrating up-regulation of both miR-27a and miR-27b in endothelial cells subjected to laminar flow (Urbich *et al.* 2012) and endothelial cells exposed to cyclic tensile strain (Wang *et al.* 2017). Downstream targets of miR-27-5p, which are known to be regulated in *in situ* cartilage explants in response to non-physiological load Al-Sabah *et al.* (unpublished data), include WNT signalling molecules such as DKK2 (Tao *et al.* 2015; Wu *et al.* 2019) and sFRP1 (Wu *et al.* 2019). Future studies will explore the relationship between mechano-sensitive miR-27-5p and downstream regulation of WNT signalling components in cartilage homeostasis.

A reduction in miR-483 levels was observed in response to non-physiological load and is the first report of its mechano-sensitivity in articular cartilage. Its potential role in cartilage homeostasis is not well defined, with conflicting evidence suggesting anabolic (Yang *et al.* 2015) and catabolic outcomes (Xu *et al.* 2017; Wang *et al.* 2019); hence, its observed reduction in response to abnormal load may reflect an attempt at tissue remodelling.

A limitation of the present study is use of immature articular cartilage removed from underlying subchondral bone, which could influence mechano-biological outcomes. However, to mitigate this limitation, we validated identified miRs in an *in vivo* model of abnormal joint loading to confirm their mechano-regulation; interestingly, many of the miRs regulated by load in our *in vitro* and *in vivo* models have also been reported to be differentially expressed in OA (Tardif *et al.* 2009; Zhang *et al.* 2014; Song *et al.* 2015; Wang *et al.* 2019), lending weight to their relevance in cartilage homeostasis.

In conclusion, the loading magnitude-dependent regulation of specific miRs identified in the present study, as well as their potential to impact on tissue homeostasis, has direct relevance to other physiological systems that are mechano-sensitive. Furthermore, it provides a pivotal mechanism by which load-induced tissue behaviours are regulated, in both health and pathology, and is critical to understand with respect to successful tissue engineering strategies in physiological systems.

References

Al-Sabah A, Stadnik P, Gilbert SJ, Duance VC & Blain EJ (2016). Importance of reference gene selection for articular cartilage mechanobiology studies. *Osteoarthritis Cartilage* **24**, 719–730.

Bader DL, Salter DM & Chowdhury TT (2011). Biomechanical influence of cartilage homeostasis in health and disease. *Arthritis* **2011**, 1.

Barter MJ, Tselepi M, Gomez R, Woods S, Hui W, Smith GR, Shanley DP, Clark IM & Young DA (2015). Genome-wide microRNA and gene analysis of mesenchymal stem cell chondrogenesis identifies an essential role and multiple targets for miR-140-5p. *Stem Cells* **33**, 3266–3280.

Buckwalter JA, Mankin HJ & Grodzinsky AJ (2005). Articular cartilage and osteoarthritis. *Instr Course Lect* **54**, 465–480.

Bustin SA, Benes V, Garson JA, Hellemans J, Huggett J, Kubista M, Mueller R, Nolan T, Pfaffl MW, Shipley GL, Vandesompele J & Wittwer CT (2009). The MIQE guidelines: minimum information for publication of quantitative real-time PCR experiments. *Clin Chem* **55**, 611–622.

Cheleschi S, De Palma A, Pecorelli A, Pascarelli NA, Valacchi G, Belmonte G, Carta S, Galeazzi M & Fioravanti A (2017). Hydrostatic pressure regulates microRNA expression levels in osteoarthritic chondrocyte cultures via the Wnt/beta-catenin pathway. *Int J Mol Sci* **18**, 133.

Crowe N, Swingler TE, Le LT, Barter MJ, Wheeler G, Pais H, Donell ST, Young DA, Dalmay T & Clark IM (2016). Detecting new microRNAs in human osteoarthritic chondrocytes identifies miR-3085 as a human, chondrocyte-selective, microRNA. *Osteoarthritis Cartilage* **24**, 534–543.

Dunn W, DuRaine G & Reddi AH (2009). Profiling microRNA expression in bovine articular cartilage and implications for mechanotransduction. *Arthritis Rheum* **60**, 2333–2339.

El-Armouche A, Schwoerer AP, Neuber C, Emons J, Biermann D, Christalla T, Grundhoff A, Eschenhagen T, Zimmermann WH & Ehmke H (2010). Common microRNA signatures in cardiac hypertrophic and atrophic remodeling induced by changes in hemodynamic load. *PLoS One* **5**, e14263.

Fehrenbacher A, Steck E, Rickert M, Roth W & Richter W (2003). Rapid regulation of collagen but not metalloproteinase 1, 3, 13, 14 and tissue inhibitor of metalloproteinase 1, 2, 3 expression in response to mechanical loading of cartilage explants in vitro. *Arch Biochem Biophys* **410**, 39–47.

Felson DT (2013). Osteoarthritis as a disease of mechanics. *Osteoarthritis Cartilage* **21**, 10–15.

Gilbert SJ & Blain EJ (2018). Cartilage mechanobiology: how chondrocytes respond to mechanical load. In *Mechanobiology in Health and Disease*, ed. Verbruggen S, pp. 99–126. Elsevier, London.

Gilbert SJ, Bonnet CS, Stadnik P, Duance VC, Mason DJ & Blain EJ (2018). Inflammatory and degenerative phases resulting from anterior cruciate rupture in a non-invasive murine model of post-traumatic osteoarthritis. *J Orthop Res* **36**, 2118-2127.

Goldring MB & Marcu KB (2012). Epigenomic and microRNA-mediated regulation in cartilage development, homeostasis, and osteoarthritis. *Trends Mol Med* **18**, 109–118.

Grodzinsky AJ, Levenston ME, Jin M & Frank EH (2000). Cartilage tissue remodeling in response to mechanical forces. *Annu Rev Biomed Eng* **2**, 691–713.

Guan YJ, Yang X, Wei L & Chen Q (2011). MiR-365: a mechanosensitive microRNA stimulates chondrocyte differentiation through targeting histone deacetylase 4. *FASEB J* **25**, 4457–4466.

Guilak F, Alexopoulos LG, Upton ML, Youn I, Choi JB, Cao L, Setton LA & Haider MA (2006). The pericellular matrix as a transducer of biomechanical and biochemical signals in articular cartilage. *Ann N Y Acad Sci* **1068**, 498–512.

Hecht N, Johnstone B, Angele P, Walker T & Richter W (2019). Mechanosensitive MiRs regulated by anabolic and catabolic loading of human cartilage. *Osteoarthritis Cartilage* **27**, 1208-1218,

Jin L, Zhao J, Jing W, Yan S, Wang X, Xiao C & Ma B (2014). Role of miR-146a in human chondrocyte apoptosis in response to mechanical pressure injury in vitro. *Int J Mol Med* **34**, 451–463.

Kilkenny C, Browne WJ, Cuthill IC, Emerson M & Altman DG (2010). Improving bioscience research reporting: the ARRIVE guidelines for reporting animal research. *J Pharmacol Pharmacother* **1**, 94–99.

Lee C, Grad S, Wimmer M & Alini M (2005). The influence of mechanical stimuli on articular cartilage tissue engineering. In *Topics in Tissue Engineering*, ed. Ashammakhi N & Reis RL, pp. 1–32. eBook. https://www.oulu.fi/spareparts/ebook_topics_in_t_e_vol2/abstracts/alini_0102.pdf

Li H, Handsaker B, Wysoker A, Fennell T, Ruan J, Homer N, Marth G, Abecasis G, Durbin R, & 1000 Genome Project Data Processing Subgroup (2009). The Sequence alignment/map (SAM) format and SAMtools. *Bioinformatics* **25**, 2078–2079.

Livak KJ & Schmittgen TD (2001). Analysis of relative gene expression data using real-time quantitative PCR and the 2(-delta delta C(T)) method. *Methods* **25**, 402–408.

Lolli A, Lambertini E, Penolazzi L, Angelozzi M, Morganti C, Franceschetti T, Pelucchi S, Gambari R & Piva R (2014). Pro-chondrogenic effect of miR-221 and slug depletion in human MSCs. *Stem Cell Rev* **10**, 841–855.

Lolli A, Narcisi R, Lambertini E, Penolazzi L, Angelozzi M, Kops N, Gasparini S, van Osch GJ & Piva R (2016). Silencing of antichondrogenic microRNA-221 in human mesenchymal stem cells promotes cartilage repair in vivo. *Stem Cells* **34**, 1801–1811.

Love MI, Huber W, Anders S (2014). Moderated estimation of fold change and dispersion for RNA-seq data with DESeq2. *Genome Biol* **15**, 550.

Luna C, Li G, Qiu J, Epstein DL & Gonzalez P (2011). MicroRNA-24 regulates the processing of latent TGFbeta1 during cyclic mechanical stress in human trabecular meshwork cells through direct targeting of FURIN. *J Cell Physiol* **226**, 1407–1414.

Martin, M. (2011). Cutadapt removes adapter sequences from high-throughput sequencing reads. *EMBnet.J* **17**, 10–12.

Mendias CL, Gumucio JP & Lynch EB (2012). Mechanical loading and TGF-beta change the expression of multiple miRNAs in tendon fibroblasts. *J Appl Physiol* **113**, 56–62.

Penolazzi L, Lambertini E, Bergamin LS, Roncada T, De Bonis P, Cavallo M & Piva R (2018). MicroRNA-221 silencing attenuates the degenerated phenotype of intervertebral disc cells. *Aging* **10**, 2001–2015.

Qin X, Wang X, Wang Y, Tang Z, Cui Q, Xi J, Li YS, Chien S & Wang N (2010). MicroRNA-19a mediates the suppressive effect of laminar flow on cyclin D1 expression in human umbilical vein endothelial cells. *Proc Natl Acad Sci U S A* **107**, 3240–3244.

Song J, Hu B, Qu H, Bi C, Huang X & Zhang M (2012). Mechanical stretch modulates microRNA 21 expression, participating in proliferation and apoptosis in cultured human aortic smooth muscle cells. *PLoS One* **7**, e47657.

Song J, Jin EH, Kim D, Kim KY, Chun CH & Jin EJ (2015). MicroRNA-222 regulates MMP-13 via targeting HDAC-4 during osteoarthritis pathogenesis. *BBA Clin* **3**, 79–89.

Tao H, Wang L, Zhou J, Pang P, Cai S, Li J, Mei S & Li F (2015). The transcription factor ccaat/enhancer binding protein beta (C/EBPbeta) and miR-27a regulate the expression of porcine Dickkopf2 (DKK2). *Sci Rep* **5**, 17972.

Tardif G, Hum D, Pelletier JP, Duval N & Martel-Pelletier J (2009). Regulation of the IGFBP-5 and MMP-13 genes by the microRNAs miR-140 and miR-27a in human osteoarthritic chondrocytes. *BMC Musculoskelet Disord* **10**, 148.

Urbich C, Kaluza D, Fromel T, Knau A, Bennewitz K, Boon RA, Bonauer A, Doebele C, Boeckel JN, Hergenreider E, Zeiher AM, Kroll J, Fleming I & Dimmeler S (2012). MicroRNA-27a/b controls endothelial cell repulsion and angiogenesis by targeting semaphorin 6A. *Blood* **119**, 1607–1616.

Wang H, Zhang H, Sun Q, Yang J, Zeng C, Ding C, Cai D, Liu A & Bai X (2019). Chondrocyte mTORC1 activation stimulates miR-483-5p via HDAC4 in osteoarthritis progression. *J Cell Physiol* **234**, 2730–2740.

Wang L, Bao H, Wang KX, Zhang P, Yao QP, Chen XH, Huang K, Qi YX & Jiang ZL (2017). Secreted miR-27a induced by cyclic stretch modulates the proliferation of endothelial cells in hypertension via GRK6. *Sci Rep* **7**, 41058.

Weber M, Baker MB, Moore JP & Searles CD (2010). MiR-21 is induced in endothelial cells by shear stress and modulates apoptosis and eNOS activity. *Biochem Biophys Res Commun* **393**, 643–648.

Wu X, Gu Q, Chen X, Mi W, Wu T & Huang H (2019). MiR-27a targets DKK2 and SFRP1 to promote reosseointegration in the regenerative treatment of peri-implantitis. *J Bone Miner Res* **34**, 123–134.

Xu R, Li J, Wei B, Huo W & Wang L (2017). MicroRNA-483-5p modulates the expression of cartilage-related genes in human chondrocytes through down-regulating TGF-β1 expression. *Tohoku J Exp Med* **243**, 41–48.

Yang M, Zhang L & Gibson GJ (2015). Chondrocyte miRNAs 221 and 483–5p respond to loss of matrix interaction by modulating proliferation and matrix synthesis. *Connect Tissue Res* **56**, 236–243.

Yang X, Guan Y, Tian S, Wang Y, Sun K & Chen Q (2016). Mechanical and IL-1beta responsive miR-365 contributes to osteoarthritis development by targeting histone deacetylase 4. *Int J Mol Sci* **17**, 436.

Zhang Y, Jia J, Yang S, Liu X, Ye S & Tian H (2014). MicroRNA-21 controls the development of osteoarthritis by targeting GDF-5 in chondrocytes. *Exp Mol Med* **46**, e79.

Zhou J, Wang KC, Wu W, Subramaniam S, Shyy JY, Chiu JJ, Li JY & Chien S (2011). MicroRNA-21 targets peroxisome proliferators-activated receptor-alpha in an autoregulatory loop to modulate flow-induced endothelial inflammation. *Proc Natl Acad Sci U S A* **108**, 10355–10360.

Additional information

Data availability statement

The data that support the findings of this study are being made openly available in GEO (GSE158571).

Competing interests

The authors declare that they have no competing interests.

Author contributions

PS, VCD, DAY and EJB were responsible for study conception and design. PS, SJG, SC, JT, AJS and EJB were responsible for data acquisition and statistical analysis. PS, SJG, SC, MJB, VCD, DAY and EJB were responsible for data analysis and interpretation. EJB was responsible for manuscript preparation. PS, SJG, SC, JT, AJS, MJB, VCD, DAY and EJB were responsible for critical revision of the draft. All authors approved the final article submitted for publication and take full responsibility for integrity of the study.

Funding

The sponsors had no role in the study design, collection, analysis and interpretation of data; in the writing of the article; nor in the decision to submit the article for publication.

Acknowledgements

This study was funded by The President's Research scholarship (Cardiff University), Versus Arthritis (18461, 19424 and 510390), the Cardiff Institute for Tissue Engineering and Repair research bursary and the JGW Patterson Foundation. Equipment was provided by the Biomechanics and Bioengineering Research Centre Versus Arthritis (18461, 510390).

Keywords

articular cartilage, *CPEB3*, mechanical load, miRNA, *TIMP3*

Supporting information

Additional supporting information may be found online in the Supporting Information section at the end of the article.

Statistical Summary Document